Chapter 5

A self similar solution for imploding shocks in non-ideal gas with gravitational effects [*]

5.1 Introduction

In this chapter, we have studied self-similar solutions of unsteady one-dimensional flow behind strong cylindrical shock waves in non-ideal gas with gravitational field having equation of state of Mie-Gruneisen type. The study of non-linear hyperbolic PDEs has long been an interesting area of research due to its practical application across various disciplines. Acceleration waves are characterized by discontinuity in normal deviates of the flow variables. Therefore, analyzing these waves is important

[*] "The contents of this chapter is ***Communicated.***"

from both mathematical and physical perspectives because of their significance in many fields like nuclear physics, uranology, seismology, particle physics, quantum mechanics, nucleonics, astronomical physics, geophysics, and different branches of engineering. Shock waves in air are small transition layers where physical properties like pressure, density and temperature change rapidly. These waves are formed by the steepening of ordinary waves, such as breakers on the shore, during the gravitational collapse of large stars leading to black holes, neutron stars and supernovae; in fluid dynamics during the process of cavitation which leads to several studies to understand the flow physics behind shock wave interactions. As the understanding of shock waves has advanced, their use for beneficial purposes has increased. For example, shock waves can be used to break kidney stones in patients by focusing on weak shock waves. They are also used to treat the tendons, ligaments, and bones of horses. Shock waves promote osteogenesis and accelerate the healing of fractures. Shock wave therapy is safe and effective, when used with proper care. Additionally, they are highly helpful in the industrial sectors, such as pencil production, wood conservation, food preservation, and sandalwood oil extraction. The authors ([161], [162], [148], [163], [103]) have employed various approaches to study the shock formation, diverging and converging shock waves and the evolutionary behavior of shock waves. Pandey and Sharma [121] examined the propagation of three-dimensional shocks by considering an infinite system of transport equations using singular surface theory. Pandey et al. [164] derived the exact solution of one dimensional system in magnetogasdynamics using invariance group properties. Bira and Sekhar [165] explored the exact solutions of isentropic flow with transverse magnetic field.

Under high pressure and temperature conditions, which are common in many shock-related scenarios, the assumption of ideal gas becomes invalid. A non-ideal gas model is the popular alternative to the ideal gas model. Wu and Roberts [115] presented the

result obtained under varying excitation conditions leading to high temperatures. For sufficiently large van der Waals excluded volume Roberts and Wu [114] found new solutions. Madhumita and Sharma [166] analyzed the evolution of shocks in non planar cases within a non-ideal medium. Using the Sakurai approch[167], Chauhan et al. [168] obtained analytical solution in non-ideal medium for planar and non-planar flows with transverse magnetic field. Anand and Yadav [169] investigated the structure of shock front and provided the exact solution of the flow field. Singh et al. [170] analyzed the evolutionary behaviour of acceleration waves and compared the obtained solution in both, ideal and non-ideal medium.

In general, finding a solution for a system of non-linear PDEs without approximations is almost not possible. According to the Rankine-Hugoniot jump conditions, the basic equation in self similar region can be solved along a set of curves, which allows the system of PDEs to be transformed into the system of ODEs ([171],[113],[95],[172]). Subsequently, various numerical approaches can be employed to solve the ODE system. Guderley [60] was the first to theoretically investigate the imploding shock waves in perfect gas. Nath [173] studied explosion problem in rotating medium for isothermal and adiabatic flows, illustrating the influence of non-ideal parameter. Using exponential law, Nath et al. [174] interpreted existence of solutions and demonstrated the effect of magnetic field, gravitational parameter and adiabatic exponent. Nath et al. [110] analyzed shock wave evolution in rotating non-ideal gas with magnetic effect. Using Lie group method, Devi et al. [175] studied evolution of shocks with monochromatic radiations in stellar interiors. For adiabatic flow, Singh [176] examined evolution of shocks with exponential and power law flows, presenting two different solution cases. The investigation of shock evolution within a mixture of non-ideal gases and small solid particles has become increasingly important owing to its numerous applications across various such as

environmental and industrial sectors. These applications encompass nozzle flow dynamics, theories related to black holes, fluid behavior in jet engines equipped with turbine blades, interactions in dusty environments following nuclear detonations, stellar formation processes, volcanic eruptions, subterranean explosions, the development of polluted crystal structures, and many more. Imploding shocks acquired great importance with the emerging possibility of achieveing matter densities well above those in charateristics of the solid state.

To find out how the flow properties behind the shock wave can be modified by deviations from the ideal gas to non-ideal gas, we have used the van der Waals gas model with gravitational field. In comparison to the Euler equation in ordinary gas dynamics, this system is more complex to find an exact analytical solution to the problem without approximation. The evolution of a strong spherical shock wave for one-dimensional unsteady flow in non-ideal dusty gas under the influence of gravitational field was investigated by J.P. Vishwakarma and G. Nath [177]. G. Nath [178] obtained similarity solutions for unsteady isothermal flow behind spherical shock wave with time dependent energy input. G. Nath [179] demonstrated the evolution of spherical shocks in non-ideal dusty gas with gravitational field. He expressed the heat conduction in terms of Fourier's law. S. Chauhan et al. [180] described the evolution of cylindrical shock waves in non-ideal gas with gravitational field using Lie group of transformation.

The current study examines the evolution of an imploding cylindrical shock waves in an unsteady, one-dimensional non-ideal gas flow, influenced by a gravitational field and described by a Mie-Gruneisen-type equation of state. The fundamental equations are reformulated into a system of first-order ordinary differential equations through the application of similarity transformation. The shock is assumed to be strong. A more comprehensive Mie-Gruneisen coefficient, denoted as $\Theta\left(\frac{\varrho}{\varrho_0}\right)$, is

integrated into the equation of state, where ϱ and ϱ_0 signify the current and initial densities of the medium, respectively. The determination of the similarity exponent, along with the flow variables, is conducted for two significant Mie-Gruneisen coefficients. The numerical approach utilized for calculating the similarity exponent is an iterative method with a single parameter, which is also applicable for deriving self-similar solutions of the second kind for shock waves induced by impulsive loads [181] in a non-ideal medium characterized by physically relevant value of Mie-Gruneisen coefficient. It is also assessed as to how the gravitational field affects the flow parameters, in non-ideal medium. We obtained numerical and approximate results for dusty gas and condensed matter under the influence of gravitational field with their defined Mie-Gruneisen cofficients. Patel et al. [182] performed an analytical evaluation of the similarity exponent for both cylindrically and spherically symmetric flows in a non-ideal medium. Additionally, Singh et al. [183] explored imploding cylindrical shocks within the context of non-ideal magnetogasdynamics. The approximate method established by Chester, Chisnell, and Whitham, known as the CCW rule [184], has proven effective in the computation of the similarity exponent. The content of the chapter is organized in the following manner: In first section, a small introduction and history of gravitational parameter are given. The system of governing equations describing one-dimensional unsteady, non-planar flow of non-ideal gas in the presence of gravitational field are presented in the second section. In third section, using new independent variables we transformed the governing equations in terms of dimensionless variables. In forth section, similarity exponents are evaluated using Chester-Chisnell-Whitham approach. Fifth section includes result and discussion part in which the similarity exponents computed using the similarity technique are compared with the similarity exponents. We discussed the numerical results and the effects of different parameters on the similarity exponent and the flow variables for two physically significant values of the Mie-Grunesian coefficient

$\Theta(D)$. Last section concludes the chapter.

5.2 Governing equations

The system of equations describing unsteady, non-planar flow of one-dimensional cylindrically symmetric motion in a non-ideal gas with gravitational field can be written in the following form (see Nath [171])

$$\begin{cases} \varrho_t + v\varrho_r + \varrho v_r + \frac{\varrho v}{r} = 0, \\ v_t + vv_r + \frac{\hat{p}_r}{\varrho} + \frac{GM}{r^2} = 0, \\ \hat{E}_t + v\hat{E}_r - \frac{\hat{p}}{\varrho}(\varrho_t + v\varrho_r)\ log(\frac{\varrho}{\varrho_0}) = 0, \end{cases} \tag{5.1}$$

where v denotes the flow velocity, t is the time, ϱ is the density, $\hat{E}$ is the specific internal energy of the medium, $\hat{p}$ is the pressure and r represents the spatial coordinate. M and G denotes the mass of the heavy nucleus at the centre([178]) and gravitational constant, respectively. The subscripts have been used for partial derivative of the flow parameters with respect to indicated variables.

The equation of state for the medium is supposed as

$$\hat{p} = \varrho E\Theta(\frac{\varrho}{\varrho_1}). \tag{5.2}$$

The Mie-Gruenisen coefficient is represented by $\Theta(\varrho/\varrho_1)$. In this context, a strong shock is presumed, and the evolution is described by the power law $R(t) \propto (1-t/t_s)^{\beta}$, where t_s denotes the collapse time, β signifies the similarity exponent, and $R(t)$ indicates the position of the shock at time t.

The conditions at the shock front, known as the Rankine-Hugoniot conditions, are as follows:

$$\varrho_2(\dot{R} - v_2) = \varrho_1 \dot{R}, \tag{5.3}$$

$$\hat{p}_2 - \hat{p}_1 = \varrho_2 v_2(\dot{R} - v_2), \tag{5.4}$$

$$\hat{E}_2 - \hat{E}_1 = \frac{\varrho_2^2}{2} + \frac{\hat{p}p_1}{\varrho_2}(1 - \frac{\varrho_1}{\varrho_2}), \tag{5.5}$$

where subscripts '1' and '2' denote the quantities ahead and behind of the shock front respectively and $\dot{R}$ is the shock speed. The conditions of strong shocks ([181]), for this problem, using (5.3)-(5.5), can be written as

$$\begin{aligned} \varrho_2 &= \varrho_1 \delta, \\ v_2 &= (1 - \frac{1}{\delta})\dot{R}, \\ \hat{p}_2 &= (1 - \frac{1}{\delta} + M_1)\varrho_1 \dot{R}^2, \end{aligned} \tag{5.6}$$

where δ is the compression across the shock wave and $M_1 = \frac{MG}{R\dot{R}^2}$ is the shock Mach number[178] referred to the frozen speed of sound $\sqrt{\frac{\gamma p_1}{\varrho_1}}$. With the help of strong shock condition (5.3)-(5.5), we can derive the relation

$$\Theta(\delta)(\delta - 1) = 2\frac{(\delta - 1 + \delta M_1)}{(\delta - 1 + 2M_1)}, \tag{5.7}$$

This equation helps us to calculate δ, once $\Theta(\varrho/\varrho_1)$ is known.

5.3 Similarity Transformation

To transform the governing equations, we introduce a new independent variable $\zeta = r/R(t)$, allowing us to set $\zeta = 1$ immediately behind the shock wave. Consequently, the field variables that characterize the flow pattern can be expressed in terms of dimensionless functions of ζ, as outlined in [185]

$v = \dot{R}V(\zeta)$, $\varrho = \varrho_1 D(\zeta)$, $\hat{p} = \varrho_1 \dot{R}^2 P(\zeta)$.

With the help of new dimensionless variables V, D, P the system (5.1) transformed to following simplified form

$$D_\zeta(\zeta - V) - DV_\zeta = \frac{iDV}{\zeta}, \tag{5.8}$$

$$V_\zeta(\zeta - V) - \frac{P_\zeta}{D} = \kappa(V + \frac{M_1}{\zeta^2}), \tag{5.9}$$

$$P_\zeta(\zeta - V) - \Phi(D)\frac{P(\zeta - V)D_\zeta}{D} = 2\kappa P, \tag{5.10}$$

where

$\Phi(D) = 1 + \Theta(D) + \frac{D}{\Theta(D)}\frac{d\Theta(D)}{dD}$ and $\kappa = 1 - \frac{1}{\beta}$.

The modified conditions for strong shock are as follows:

$$\begin{aligned} V(1) &= 1 - \delta, \\ D(1) &= \frac{1}{\delta}, \\ P(1) &= 1 - \delta. \end{aligned} \tag{5.11}$$

The transformed equations (5.8) to (5.10) represent nonlinear ordinary differential equations, for which an analytical solution cannot be obtained. Consequently, these equations are addressed through numerical methods. Since the relative particle velocity of the shock front is subsonic, specifically $(v_2 - \dot{R})^2 < C^2$, where C denotes the sound speed at the shock. Also, condition on $\Theta(D)$ can be derived using (5.9) as $\frac{d}{dD}[\frac{2}{\Theta(D)}] < 1$ at $D = \delta$. Now, from (5.8)-(5.10), we have

$$D_\zeta = \frac{2\kappa PD\zeta + D^2(\zeta - V)\zeta(\kappa V + \frac{M_1}{\zeta^2}) + iD^2V(\zeta - V)^2}{\zeta(\zeta - V)((\zeta - V)^2 D - \Theta(D)P)}, \tag{5.12}$$

$$V_\zeta = \frac{2\kappa P\zeta + PiV\Theta(D) + i\zeta D^2(\zeta - V)^2(\kappa V + \frac{M_1}{\zeta^2})}{\zeta((\zeta - V)^2 D - \Theta(D)P)}, \tag{5.13}$$

$$P_\zeta = PD\frac{[\Theta(D)\zeta(\kappa V + \frac{M_1}{\zeta^2}) + iV\Theta(D)(\zeta - V) + 2\kappa\zeta(\zeta - V)]}{\eta((\zeta - V)^2 - \Theta(D)P)}. \tag{5.14}$$

For a specified Mie-Gruneisen coefficient, the compression δ is initially determined using equation (5.7). Subsequently, equations (5.12) to (5.14) are integrated from $\zeta = 1$, applying the conditions outlined in (5.11), utilizing the Runge-Kutta method with an arbitrary value of β. By employing the parameter (β), we determined the corrected value of β using iterative process. In order to get non-singular solution of equation (5.12)-(5.14), we choose exponent β such that denominators of D_ζ, V_ζ, P_ζ vanishes at those points where its numerator vanishes, in the domain of interest $1 < \zeta < \infty$ and that will be the singular point of the system. The appropriate value of β yields the final non-singular solutions. This approach has proven to be highly effective in obtaining self-similar solutions of the second kind for imploding shocks in non-ideal media, as referenced in [182], regardless of the Mie-Gruneisen coefficient.

5.4 Approximate Method

In this part, we evaluate the similarity exponent using CCW rule, often known as approximate method ([1]). The differential equation for $\hat{p_2}$ in terms of R is expressed using this rule as

$$\frac{d\hat{p_2}}{dR} + \varrho_2 c_2 \frac{dv_2}{dR} + \frac{\varrho_2 c_2^2 v_2}{R(v_2 + c_2)} + \frac{\varrho_2 G M_1 c_2}{R^2(v_2 + c_2)} = 0 \tag{5.15}$$

The speed of sound immediately behind the shock is denoted by $c_2 = \sqrt{\frac{p_2}{\varrho_2}\Phi(\frac{\varrho_2}{\varrho_1})}$. Using the strong shock conditions (5.6), we can reduce equation (5.15) to

$$\frac{R\ddot{R}}{\dot{R}^2} + \frac{1}{T} = 0, \tag{5.16}$$

where $T = \frac{(1-\frac{1}{\delta}+Q)(1-\frac{1}{\delta})(2+\delta Q+2M_1)}{m\delta(Q^2(1-\frac{1}{\delta}))+\delta M_1 Q}$, and $Q = \sqrt{\frac{\Phi(\delta)((1-\frac{1}{\delta})+M_1)}{\delta}}$.

Solving (5.16) we get,

$$R \propto (1 - \frac{t}{t_s})^{\beta}, \qquad \beta = \frac{T}{T+1} \tag{5.17}$$

For the case $M_1 = 0$, Q and T becomes $Q = \sqrt{\frac{\Phi(\delta)(1-\frac{1}{\delta})}{\delta}}$ and
$T = \frac{1}{\Phi(\delta)}\left[1 + \sqrt{\frac{\Phi(\delta)}{\delta-1}}\right]\left[2 + (\delta-1)\sqrt{\frac{\Phi(\delta)}{\delta-1}}\right]$.
which is same as results obtained in Mie-Gruenisen type non-ideal medium[182].

5.5 Results and discussion

Two physically significant values of the Mie-Grunesian coefficient $\Theta(D)$ have been calculated numerically and are provided below:

i) If Mie-Gruenisen coefficient is taken this way, then the equation of state of the dusty gas can be written as ([53])

$$\Theta(D) = \frac{K-1}{1-Z_0 D}, \tag{5.18}$$

where Z_0 and K are the initial volume fraction of solid particles and ratio of specific heat of dusty gas. Using equation (5.18) in (5.7), we get a quadratic equation in terms of δ

$$\delta^2(K-1+2Z_0(1+M_1))+2\beta(M_1(K-1)-K-M_1-Z_0)+K+2M_1(1-K)+1=0. \tag{5.19}$$

The quadratic equation (5.19) is solved numerically. In our subsequent computations, we have simply used physically meaningful values of δ.

We obtained values of similarity exponent numerically i.e β_n as well as approximately i.e β_c, for K = 1.4, $\gamma = 4/3$ and various values of Z_0 are displayed in Table 5.1. The density, velocity and pressure profile for $K = 1.4$ and $Z_0 = 0.004, 0.01, 0.02, 0.1$ are shown in Fig. 5.1, 5.2 and 5.3.

TABLE 5.1: For $K = 1.4$, $\gamma = 4/3$ and $M = 4$, the similarity exponents for a dusty gas with gravitational field

Z_0	δ	β_n	β_c
0.0	1.53164	0.658214	0.67067
0.001	1.5311	0.65777	0.670549
0.005	1.52895	0.656034	0.670062
0.01	1.52627	0.653729	0.669452
0.02	1.52091	0.650524	0.668226
0.04	1.51023	0.646653	0.665751
0.06	1.49961	0.640425	0.663245
0.08	1.48903	0.635305	0.660707
0.1	1.4785	0.630393	0.658137

TABLE 5.2: For $K = 1.4$, $\gamma = 1.4$ and $M = 5$, the similarity exponents for a dusty gas with gravitational field

Z_0	δ	β_n	β_c
0.0	1.53164	0.678199	0.696201
0.001	1.41001	0.678085	0.696087
0.005	1.40856	0.681141	0.695631
0.01	1.40674	0.680714	0.69506
0.02	1.40311	0.677924	0.693911
0.04	1.39585	0.673522	0.69159
0.06	1.3886	0.674198	0.689236
0.08	1.38135	0.667986	0.686848
0.1	1.3741	0.660499	0.684426

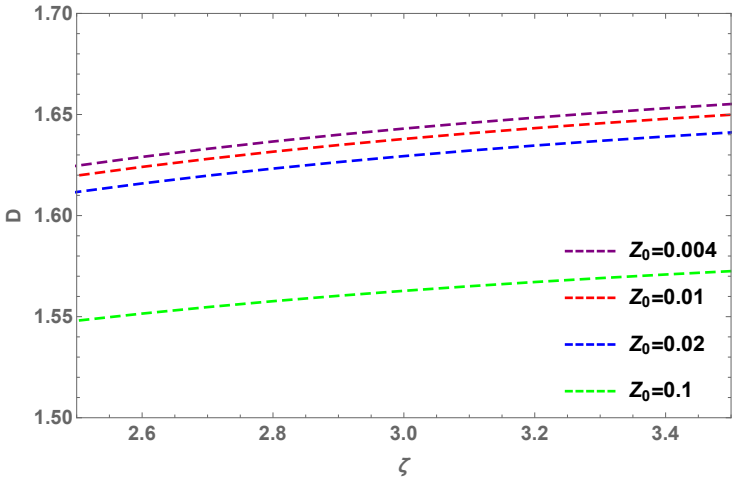

FIGURE 5.1: Density profile for K= 1.4, M=5, $Z_0 = 0.004,\ 0.01,\ 0.02,\ 0.1$ and $\gamma = 1.4$

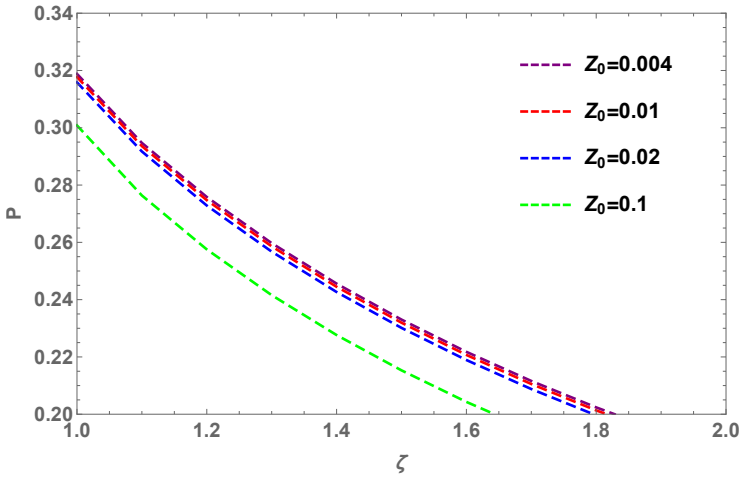

FIGURE 5.2: Pressure profile for K= 1.4, M=5, $Z_0 = 0.004,\ 0.01,\ 0.02,\ 0.1$ and $\gamma = 1.4$

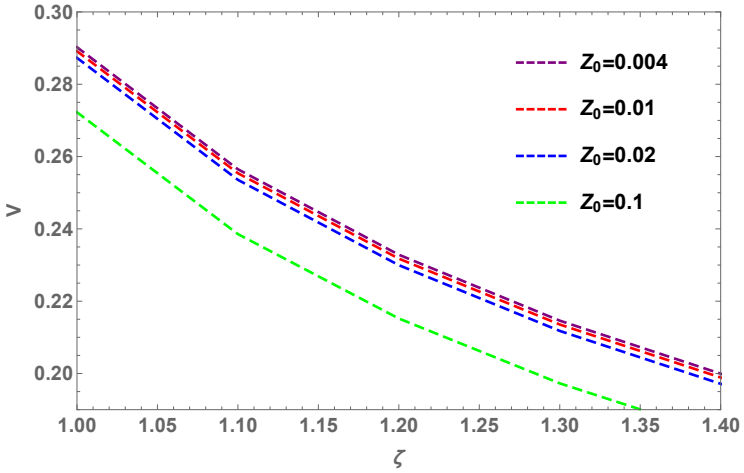

FIGURE 5.3: Velocity profile for K= 1.4, M=5, $Z_0 = 0.004,\ 0.01,\ 0.02,\ 0.1$ and $\gamma = 1.4$

ii))The following is the Mie-Gruenisen coefficient for condensed matter([186])

$$\Theta(D) = \frac{2}{3} + \left(\Theta_0 - \frac{2}{3}\right)\frac{D_m^2 + 1}{D_m^2 + D^2}D, \tag{5.20}$$

where the parameters D_m and Θ_0 are usually determined by experiment. A bi-quadratic equation in terms of δ is obtained by using (5.20) in (5.7) as

$$2(1+2M_1)\delta^4 + \delta^3 P_1 + \delta^2 P_2 + P_3\delta + 8D_m^2 = 0. \tag{5.21}$$

where $P_1 = -4M_1 - 4 + 3A(1+2M_1) - 6(1+M_1)$,

$P_2 = 2 + 2D_m^2(1+2M_1) - 6A(1+M_1) + 6$,

$P_3 = -4D_m^2(1+M_1) + 3A - 6D_m^2(1+M_1)$,

$A = (\Theta_0 - \frac{2}{3})(D_m^2 + 1)$.

For perfect gas Θ_0=2/3 and the value of P_1, P_2 and P_3 reduces to $-4-4M_1-6(1+M)$, $8+2D_m^2(1+2M_1)$ and $-10D_m^2(1+M_1)$ respectively. Two real and two complex roots are obtained here. The roots having physical significance are retained. For iron, copper, and aluminum, the values of the parameter Θ_0 are 1.78, 2.02, and 2.19, respectively, with the range of $0.5 \leq D_m \leq 0.8$. The equations (5.19) and (5.21) are used to determine the values of δ for various parameters including K, Z_0, Θ_0, D_m, $\gamma = 1.4$, 4/3, and $M = 4$, 5, which are detailed in Tables 5.1 through 5.4. It is important to highlight that for both values of $\Theta(D)$ in non-ideal media which is

TABLE 5.3: For $\gamma = 4/3$ and $M = 5$, the similarity exponents for condensed matter with gravitational field

Θ_0	D_m	δ	β_n	β_c
1.78	0.5	2.62149	0.640211	0.641605
	0.65	2.52057	0.6372719	0.639075
	0.8	2.41475	0.629508	0.635464
2.02	0.5	2.42902	0.636894	0.638779
	0.65	2.32872	0.626192	0.635088
	0.8	2.22762	0.6187872	0.630291
2.19	0.5	2.30947	0.622743	0.636143
	0.65	2.21233	0.612591	0.631732
	0.8	2.11682	0.604138	0.626296

TABLE 5.4: For $\gamma = 1.4$ and $M = 4$, the similarity exponents for condensed matter with gravitational field

Θ_0	D_m	δ	β_n	β_c
1.78	0.5	2.5777	0.6241103	0.625237
	0.65	2.47872	0.6222763	0.623197
	0.8	2.37535	0.618322	0.620131
2.02	0.5	2.38752	0.6218401	0.623292
	0.65	2.2896	0.6183869	0.62011
	0.8	2.19133	0.614476	0.615871
2.19	0.5	2.26968	0.619418	0.621206
	0.65	2.17515	0.6075091	0.617309
	0.8	2.0826	0.599825	0.612432

influenced by a gravitational field, the values of the similarity exponent decreases as the corresponding influencing parameters of the medium increases. The flow variable profiles are calculated using the fourth-order Runge-Kutta method for $1 \leq \zeta < \infty$ based on equations $(5.12 - 5.15)$, adhering to the boundary conditions outlined in (5.11). The characteristics of the flow profiles are depicted in Figures 5.1 to 5.6 for the parameters $K = 1.4$, $Z_0 = 0.004,\ 0.01,\ 0.02,\ 0.1$, $\Theta_0 = 1.78$, $D_m = 0.5$, $\gamma = 4/3$, and $M = 5$. It is noteworthy that the scenario where $M_1 = 0$ pertains to a non-gravitational case, thereby aligning with the findings of [182]. Figures 5.1 to 5.3 illustrate that the absolute values of the flow variables decreases as the parameter Z_0 increases in a non-ideal medium with gravitational field i.e. with the increase in the value of volume fraction of dust particles, the trend of the profiles of flow variables show the decaying behavior. Where as completely opposite effect is observed in condensed matter case which is evident from figures 5.4 to 5.6 . As the parameters Θ_0, and D_m increases in a non-ideal medium under the influence of a gravitational field, the density, pressure and velocity profile steepens after a finite time. Additionally, the results presented in Tables 5.1–5.4 indicate that the CCW method yields a highly accurate approximation for similarity exponents in non-ideal media affected by a gravitational field in both cases i.e. in dusty gas and

in condensed matter.

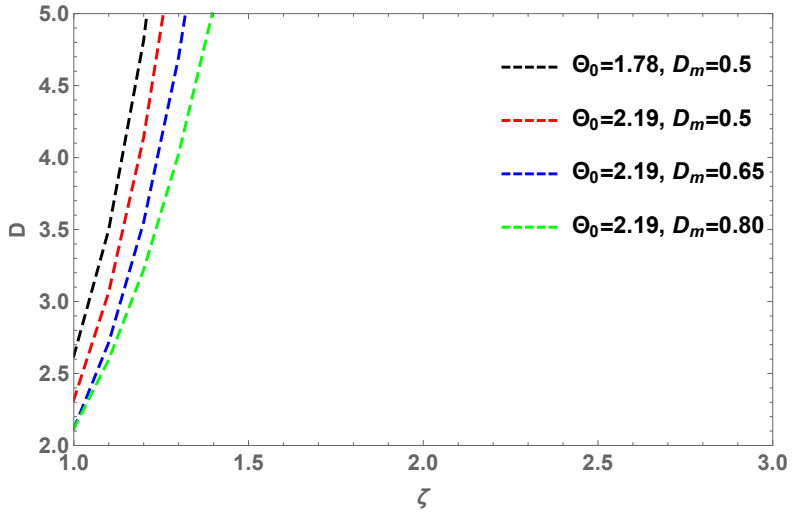

FIGURE 5.4: Density profile for $\gamma = 4/3$, $M = 5$, $\Theta_0 = 1.78,\ 2.19,\ 2.19\ 2.19$, $D_m = 0.5,\ 0.5,\ 0.65,\ 0.80$

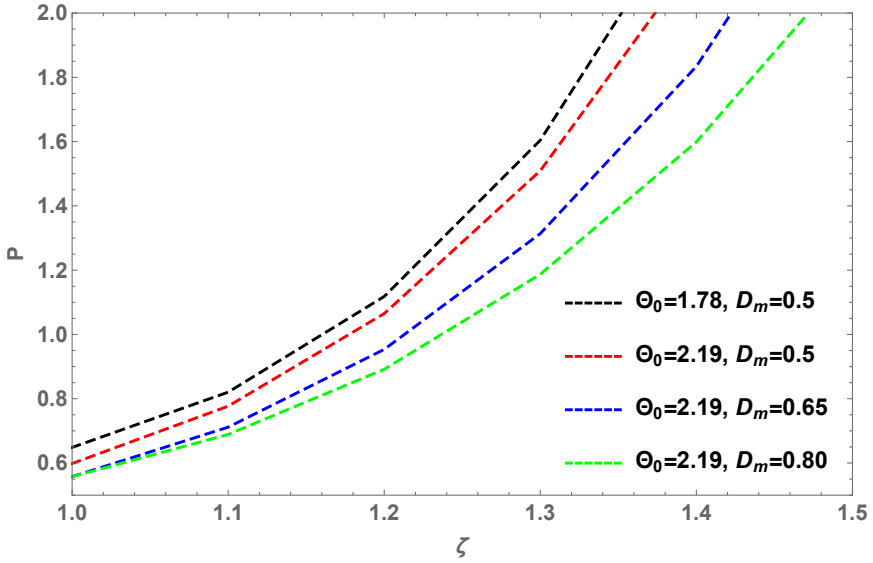

FIGURE 5.5: Pressure profile for $\gamma = 4/3$, $M = 5$, $\Theta_0 = 1.78,\ 2.19,\ 2.19\ 2.19$, $D_m = 0.5,\ 0.5,\ 0.65,\ 0.80$

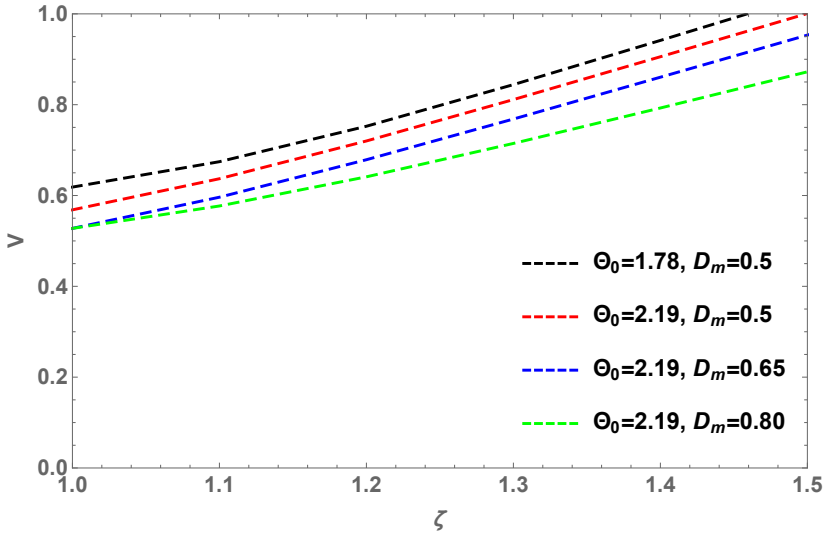

FIGURE 5.6: Velocity profile for $\gamma = 4/3$, $M = 5$, $\Theta_0 = 1.78,\ 2.19,\ 2.19\ 2.19$, $D_m = 0.5,\ 0.5,\ 0.65,\ 0.80$

5.6 Conclusion

The technique of similarity solutions of the second kind is utilized to determine the similarity exponent and the flow parameter distribution behind the wave front moving through a non-ideal medium with the influence of gravitational field. It is assumed that the equation of state for the non-ideal medium is of Mie-Gruneisen type. A comparative study is performed between the numerical approach and the CCW approximation technique for a non-ideal medium within a gravitational field. Solutions to the system of nonlinear ordinary differential equations are numerically obtained to evaluate the distribution of flow parameters, including density, velocity, and pressure, for two distinct and physically relevant non-ideal media: dusty gas and condensed matter. It is noted that the values of the similarity exponent decreases as the concentration of dust particles and condensed material increases. Graphical representations of the profiles of density, velocity, and pressure are presented. As the value of Z_0 increases, the presence of dust particles rises, leading to a reduction in

shock speed, density, and pressure, as seen in the graphs. While in case of condensed matter, there is steeping in the profile of flow variables. The issue addressed in this study is related to fusion research, the methodology and analysis presented could be relevant to many other physical systems governed by nonlinear hyperbolic partial differential equations.

****